

Scattering from *Rhizophora* spp. Particleboards

N. Syazwina^{1, 3*}, S. Bauk², A. A. Tajuddin³ and A. Shukri³

¹*Radiography Programme, Faculty of Medicine & Health Sciences, Universiti Sultan Zainal Abidin, Jalan Sultan Mahmud, 20400 Kuala Terengganu, Terengganu, Malaysia.*

²*Physics Section, School of Distance Education, Universiti Sains Malaysia, 11800 Penang, Malaysia.*

³*School of Physics, Universiti Sains Malaysia, 11800 Penang, Malaysia.*

* *nurulsyazwina@unisza.edu.my*

Abstract. *Rhizophora* spp. has the potential to be a tissue equivalent material as it has the same radiological properties found in water and tissues. Ten types of particleboards fabricated from two particle sizes and different percentages of resins designated as Particle A: PF 8%, UF 8%, UF 13%, PRF 13%, PF 13% and Particle B: PF 8%, UF 8%, UF 13%, PRF 13%, PF 13% were used in a 0°, 7°, 20°, 45°, and 70° Compton scattering arrangement using an Am-241 source and a Nal (Tl) detector system. Channel shift, measured scattered photon energy and intensity (count per second) was evaluated for scattering properties compared with water. Results showed that channel shift was almost constant at 0° – 20° angle of scattering which was around 387 - 391 channel number and started to reduce simultaneously from 370 - 387 channel numbers at 20° until 70° for all samples including water. All particleboards exhibit the same pattern of measured scattered photon energy with water. On the other hand, all of the samples showed exponential relationship of count per second for angle of scattering from 7° to 70°. As for conclusion, all types of particleboards have the same scattering properties as their channel shift, measured scattered photon energy, and count per second were almost same to each other as well as to water. Thus, we can say that these particleboards have the potential to become as water equivalent materials after considering the limitations in this study.

I. INTRODUCTION

Rhizophora spp. particleboards might have the potential to be a new phantom material. Interest in this material was aroused as efforts have been made to study its mass attenuation coefficients and was found to be potentially water-equivalent. However, not much had been done on the investigation of photon scattering from such materials although scattering may have importance in simulations which have yet to be explored [1].

It is not always practical to perform dosimetric measurements in a water phantom as it poses some practical problems when used in conjunction with ion chambers and other detectors that are affected by water, unless they are designed to be waterproof [2]. In addition, measurements within high dose gradients can be difficult to perform in water [3,4]. Hence, solid homogeneous phantoms such as polystyrene, acrylic and phantoms made from proprietary materials have found considerable popularity, particularly for clinical dosimetry. Ideally, for a given material to be tissue or water equivalent, it must have the same radiological properties as that of water which includes the effective atomic number, the number of electrons per gram and the mass density [5,6].

However, since Compton Effect is the most predominant mode of interaction for megavoltage photon beams in the clinical range, the necessary condition for water equivalence for such

beam is the same electron density as that of water [7]. On the other hand, photons produced by therapeutic kilovoltage X-ray units and some brachytherapy sources are lower in energy and photoelectric effect becomes a more dominant interaction process. This means that at these lower energies, differences in the effective atomic number of the solid phantom as compared to water may lead to greater differences in measured dose [7]. Thus, implementation of other phantom is needed in order to compensate those problems. One of the potential phantom materials is *Rhizophora* spp. wood phantom which was found to be water equivalent [1,8,9].

Rhizophora spp. may be shredded into particles and compressed into particleboards using adhesives and additives in order to overcome the decaying of untreated raw *Rhizophora* spp. by bacteria, fungi or insects. It also may become cracked and warped with time. Furthermore, it is difficult to build up needed size of *Rhizophora* spp. phantom due to the limited diameter size of *Rhizophora* spp. tree trunk, which is typically less than 25 cm. Particleboard is a type of fiberboard, a composite material, but it made up of larger pieces of wood particles. In the present study *Rhizophora* spp. particleboard samples were used in conjunction with a single source low energy technique, utilizing the 59.54 keV photon emission of Am-241 to obtain the scattering profiles. It is based on analyzing the angular position, the intensity, and the peak shape of the scattered radiation [10]. In order to be considered a tissue-equivalent material, the scattering profiles of the fabricated *Rhizophora* spp. particleboards should be comparable to that of tissue. So, finding all of the properties is crucial in order for *Rhizophora* spp. to become a standard phantom. The aim of the present study is to study the scattering properties of gamma rays from the *Rhizophora* spp. particleboards.

II. MATERIALS AND METHODS

The *Rhizophora* spp. particleboard samples were fabricated by a previous researcher [11]. During fabrication of the particleboards, *Rhizophora* spp. wood had been shredded into particles and compressed into particleboards using Phenol formaldehyde (PF), Urea formaldehyde (UF), or Phenol resorcinol formaldehyde (PRF) as adhesives. It is manufactured by mixing wood particles or flakes together with a resin and forming the mix into a sheet. The raw material to be used for the particles is fed into a disc chipper with between four and sixteen radially arranged blades. Choosing the right particle size is important in order to fabricate the particleboard which exactly mimicking the standard phantom. So, the particleboards that were fabricated with different particle sizes will be differentiating in term of scattering properties in order to study which particle sizes closely mimicking the standard phantom. In this study, large size particles: Particle A were produced by using grinder sieve with 5 mm diameter holes while small size particles: Particle B were produced by using grinder sieve with 3 mm diameter holes. The particles are first dried, after which any oversized or undersized particles are screened out. Resin, in liquid form, is then sprayed through nozzles onto the particles. These resins are sometimes mixed with other additives before being applied to the particles, in order to make the final product waterproof, fireproof, insect proof, or to give it some other qualities. Once the resin has been mixed with the particles, the liquid mixture is formed into a sheet. A weighing device notes the weight of flakes, and they are distributed into position by rotating rakes. The sheets formed are then cold-compressed to reduce their thickness and make them easier to transport. Later, they are compressed again, under pressures between two and three megapascals and temperatures between 140 °C and 220 °C. This process sets and hardens the glue. All aspects of this entire

process must be carefully controlled to ensure the correct size, density and consistency of the board. The boards are then cooled, trimmed and sanded. They can then be sold untreated, or covered in a wood veneer. [11]

Measurements were performed using a NaI(Tl) scintillation detector Bicon Model 2M2 connected to an ORTEC 570 amplifier and a multi-channel analyzer (MCA). A 45 mCi Am-241 point source was used. The Am-241 source can be revolved around the sample at different scattering angles, θ . A pin-hole collimator was put in between the point source and the sample to allow only a well collimated photon beam to be incident on the sample. Another collimator was placed between the sample and the detector. The set-up is as shown in Figure 1 and was aligned by using a laser beam.

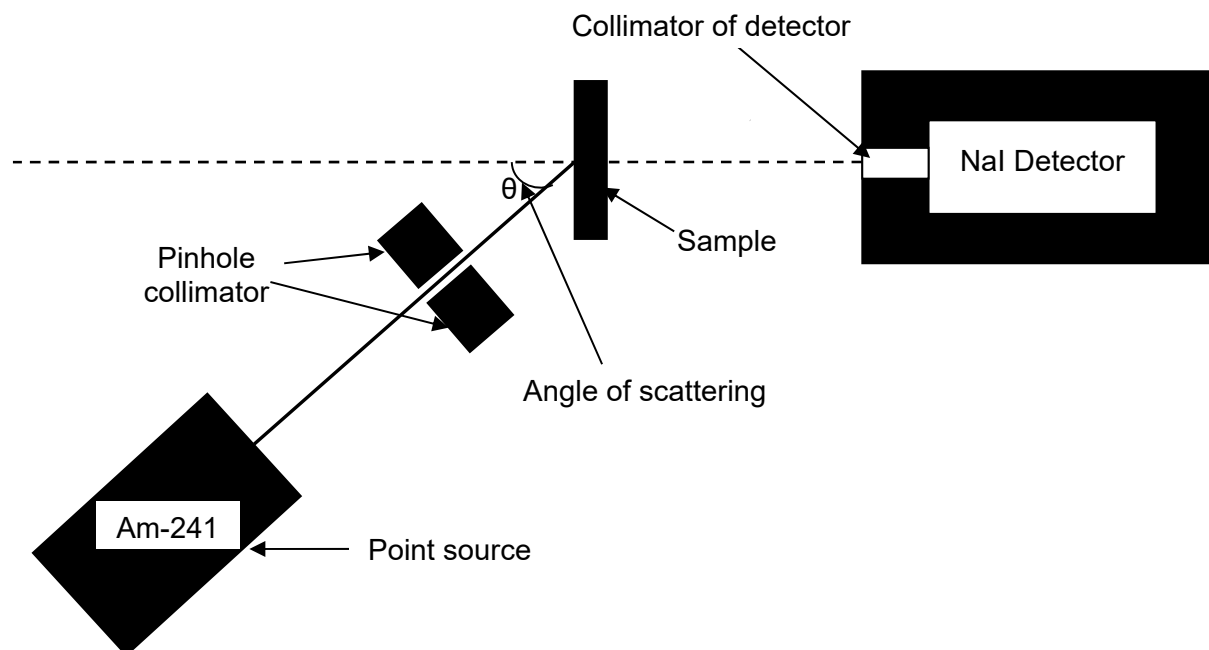


Fig. 1: Experimental set up for scattering study.

Ten samples, each 0.5 cm thick and plane size 21 x 21 cm², of *Rhizophora* spp. particleboards were labelled as Particle A (large size particles) and Particle B (small size particles); at different treatment levels of Phenol formaldehyde 8 % (PF 8%), Urea formaldehyde 8 % (UF 8%), Urea formaldehyde 13 % (UF 13%), Phenol resorcinol formaldehyde 13 % (PRF 13%), and Phenol formaldehyde 13 % (PF 13%) (Table 1).

Table 1: Table of the abbreviation used in this study for different types of *Rhizophora* spp. particleboards sample.

Resin type	Resin treatment level	Particle A	Particle B
Phenol formaldehyde (PF)	8%	A:PF 8%	B:PF 8%
	13%	A:PF 13%	B:PF 13%
Urea formaldehyde (UF)	8%	A:UF 8%	B:UF 8%
	13%	A:UF 13%	B:UF 13%
Phenol resorcinol formaldehyde (PRF)	13%	A:PRF 13%	B:PRF 13%

A water phantom was made by putting water in a fabricated Perspex container. The effective size of the water sample was $15 \times 8 \times 1 \text{ cm}^3$. The scattered photon spectrum due to water was obtained by subtracting spectrum due to the empty container from the spectrum due to water and container. Then, each of the samples was placed at about 14.5 cm in front of the detector. Scattering angles of 0° , 7° , 20° , 45° , and 70° were used. The detector live time was set at 900 seconds for 0° , 14400 seconds for 7° , 28800 seconds for 20° , 50400 seconds for 45° and 72000 seconds for 70° .

III. RESULTS AND DISCUSSIONS

A. Energy Calibration

Table 2 show the channel position and the corresponding energy for the two peaks which are at 27.03 and 59.63 keV base on the spectrum in Figure 2 after performing the calibration procedure. Base on Figure 3 we can see that higher channel number will give higher photon energy.

Table 2: The energy and channel position for the two peaks detected in Am-241 spectrum.

Peak	Energy (keV)	Channel number
1	27.03	253
2	59.63	389

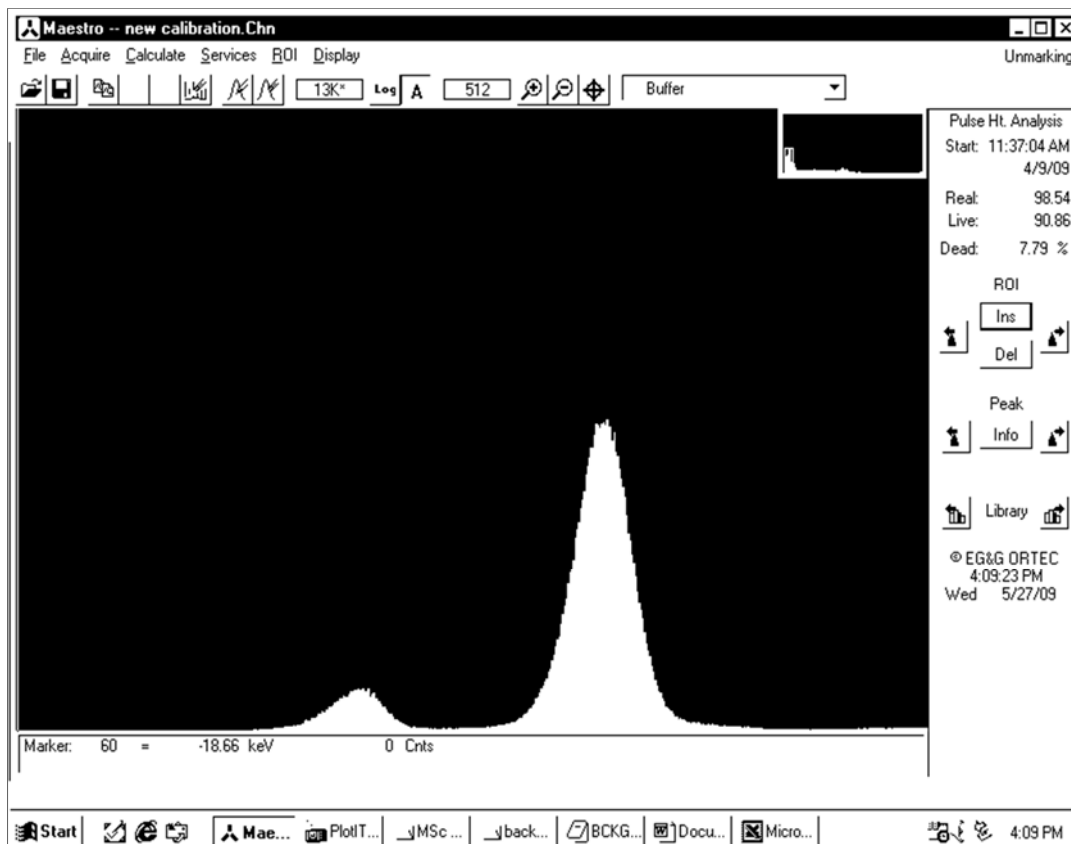


Fig. 2: Spectrum of Am-241 detected by our NaI(Tl) detector.

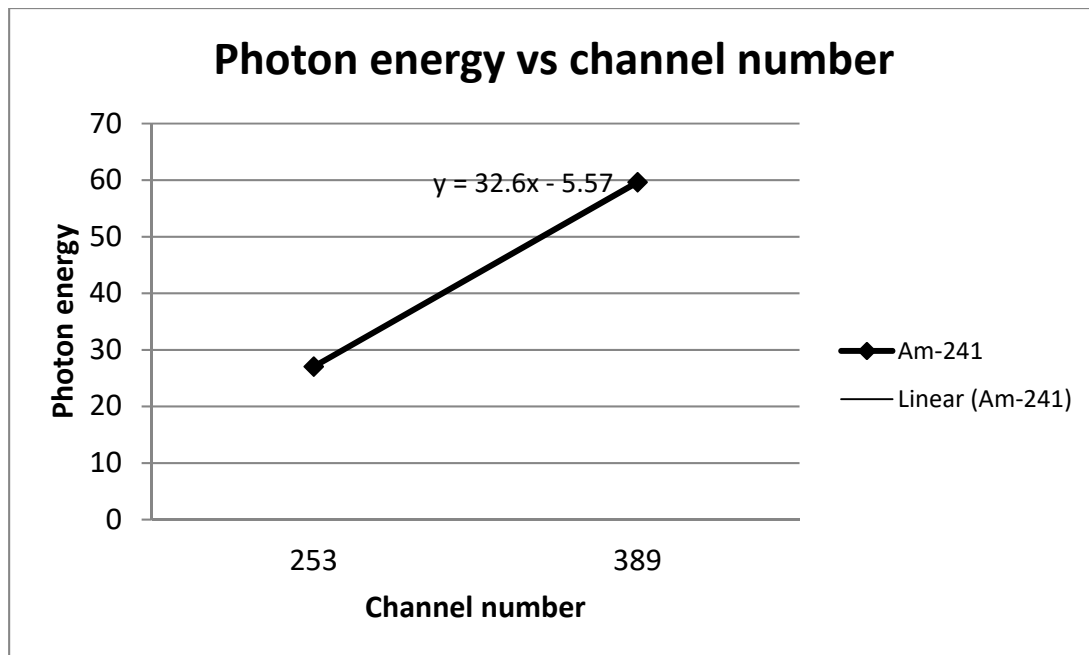


Figure 3: Calibration curve which showing channel number versus photon energy of Am-241.

B. Shape of the peaks (Appendix A)

The main characterizing features of any scattered spectrum are well resolved spectrum, good intensity and appropriate identifying information [12]. In this study, the scattered γ -ray spectra from different particleboards samples showed various peaks including scattered peaks (coherent and incoherent), sum peaks, and I escape peaks. The elastic scattered peaks of 59.54 keV and 26.36 keV were clearly resolved from their Compton peaks for all samples at 0°. However, at 7°, 20°, 45° and 70°, only 59.54 keV of elastic scattered peak clearly seen but there is small overlap with the background radiation before subtraction especially at large angle of scattering. Otherwise, peak of 26.36 keV was vaguely seen at small scattering angle and become disappear with increasing angle of scattering. All curves for all samples at certain angle (from 0° till 70°) show basically the same shape, with the main peak in the same position, but with different height, being higher for water except at 0°. As the angle increases from 0° to 70°, the height of the main peak (at 59.54 keV) for all samples decreases and background radiation increases with duration of counting where it's slowly exhibit a peak just after the main peak. But, after subtraction of the background count using Microsoft Excel, peak of the background slightly disappear. Increasing the angle of scattering also causing the position of the main peak shifted to the lower channel number.

C. Channel shift

The energy shift depends on the angle of scattering and not on the nature of the scattering medium. This can be proved by the equation (1) stated in Section 3.4 where energy of the scattered photons is dependent on the angle of scattering, θ . Shift in energy will also shift in channel number as there is relationship between energy and channel number. Based on this study, increasing the angle of scattering from 0° till 70° will decreases the energy and channel shift for all samples including water. Large angle of scattering shifted the energy more than low angle of scattering because for small scattering angle θ , the predominant interaction is coherent scattering whereas for large scattering angle the predominant interaction is Compton

interaction. Since the scattered x-ray photon has less energy, it, therefore, has a longer wavelength than the incident photon. Thus, very little energy transferred to the electron in coherent scattering produce scattered photon with more energy left causes only small channel or energy shift at low angle of scattering. Whereas, more energy transferred to electron in Compton interaction produce scattered photon with less energy left causes quite larger channel or energy shift for large scattering angle. That is why there is only a little channel shift or almost no channel shift at 0° to 20° for Particle A except PRF 13% shows a small fluctuation from the initial channel position at 0°. Otherwise, quite larger channel shift occur at 20° till 70° for all samples of Particle A where its decreases monotonically within the range of 389 - 370 channel number as shown in Figure 4.

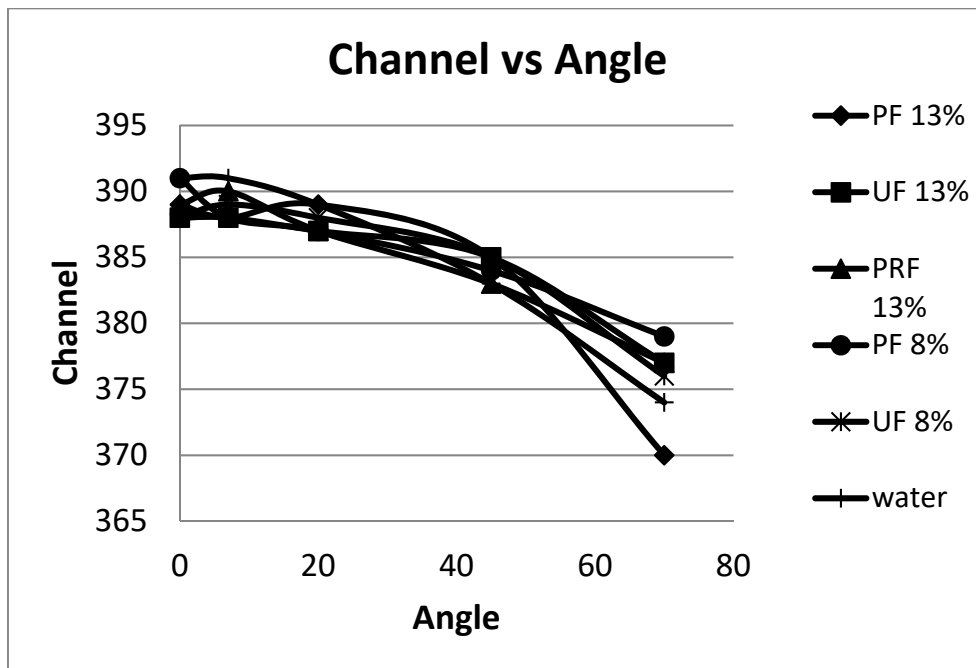


Fig. 4: Graph of channel shift with increasing angle of scattering for all of Particle A compared with water.

For Particle B, there is almost no channel shift for low angle of scattering where its produce a constant channel position at the main peak of 0° till 20° angle of scattering which is around 388 to 391 channel number as shown in Figure 5. But, for PF 8% it's fluctuate from 389 to 390 and lastly to 387 channel number, however channel shift for large angle scattering is almost same as Particle A as shown in Figure 5. For water, channel shift was uniform at 0 ° to 70 ° angle of scattering which is within a narrow range of 374 – 391 channel number.

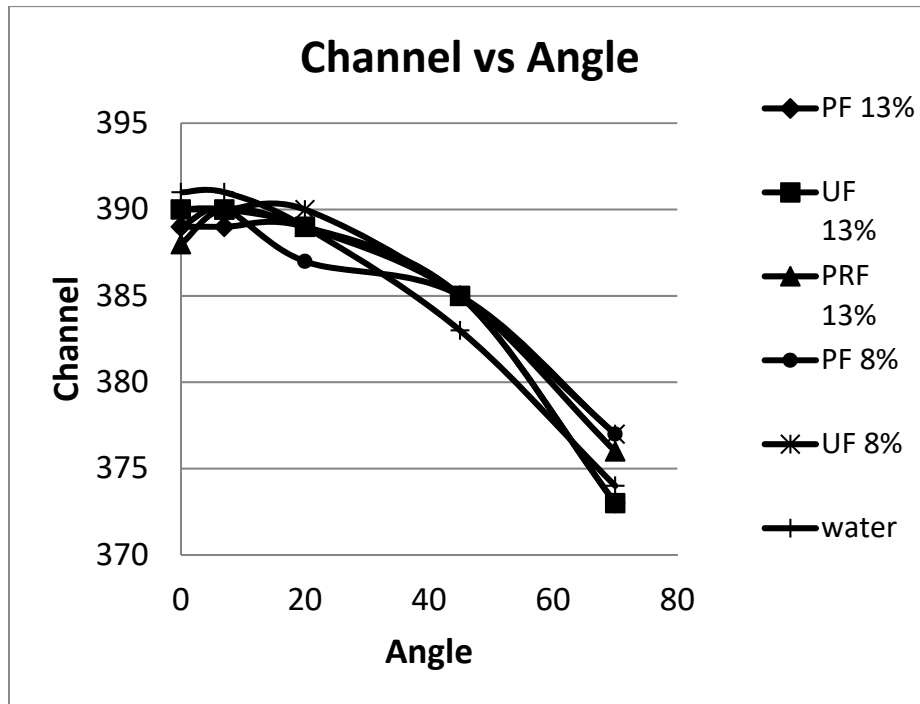


Fig. 5: Graph of channel shift with increasing angle of scattering for all of Particle B compared with water.

C. Measured and calculated scattered photon energy

The measured scattered photon energy was compared with the scattered photon energy calculated by the equation [2]

$$E'_\gamma = \frac{E_\gamma}{1 + \left(\frac{E_\gamma}{mc^2}\right)(1 - \cos\theta)} \tag{1}$$

The value of measured scattered photon energy was almost same with the calculated scattered photon energy shown in Table 3 at 0° till 20 ° angle of scattering except for Particle B: UF 8% and water where the measured scattered photon energy was always higher than calculated scattered photon energy.

Table 3: Table of the calculated scattered photon energy with increasing angle of scattering.

Angle (°)	Calculated energy (keV)
0	59.54
7	59.49
20	59.12
45	57.58
70	55.30

Both the measured and calculated scattered photon energy firstly was almost constant but it started to decrease uniformly at 20°. There is small deviation between the measured and

calculated scattered photon energy which is only less than 3.3 %. But, the deviation is more in Particle A than in Particle B for all types of resin materials. It may due to the larger particle size shift the channel number more than the smaller particle size because more energy transfers to larger particle than the smaller particle to eject the electron of Rhizophora spp. particleboards which causes lower energy deflected photon detected.

For Particle A, the measured and calculated scattered photon energy is the same for all types of resin materials at low angle of scattering (0° to 20°) except for PF13% but there is small deviation of measured value from the calculated scattered photon energy for the large angle of scattering (at 45° and 70°) (Figure 6).

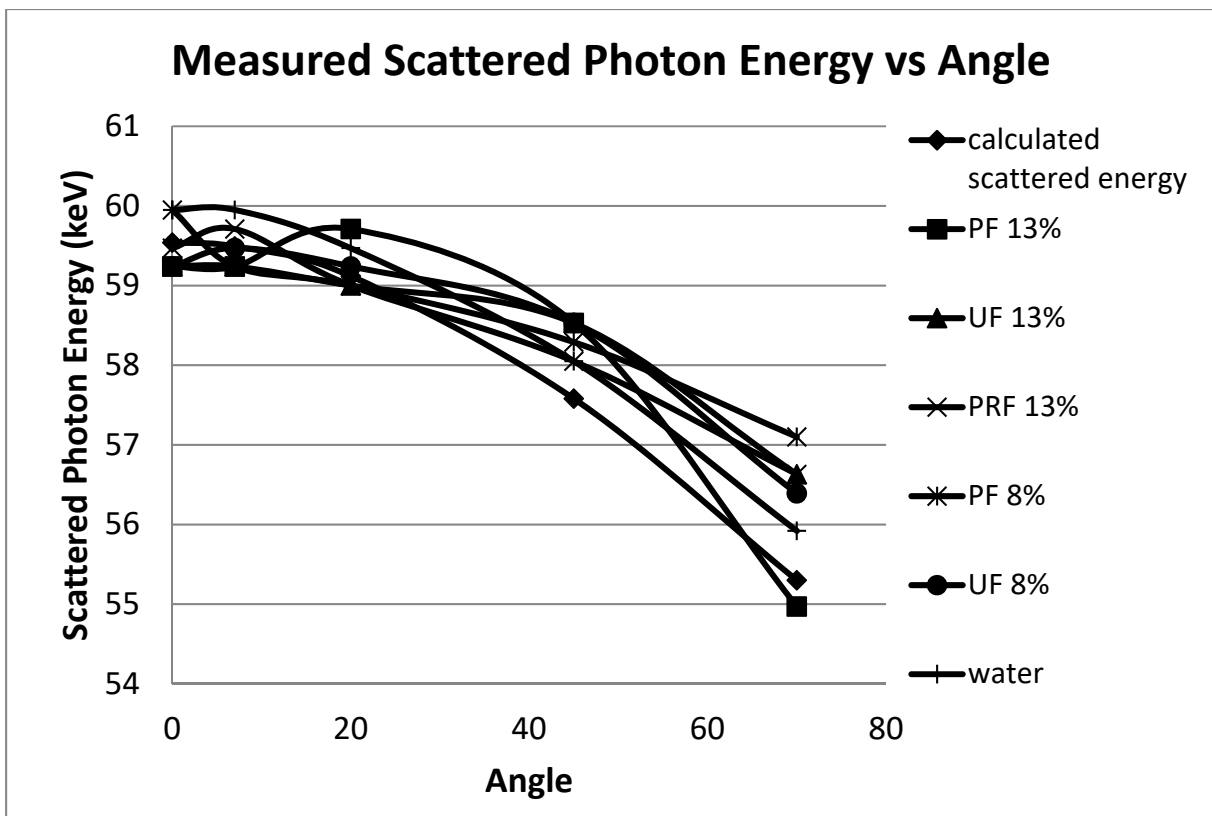


Fig. 6: Graph of measured scattered photon energy with increasing angle of scattering for all of Particle A compared with water.

For Particle B, the measured scattered photon energy is always higher than the calculated scattered photon energy. For small scattering angle, the deviation is only small rather than larger in large scattering angle. Otherwise, measured scattered photon energy for water was always higher than calculated scattered photon energy which is about ~0.59% - 1.12% more. However, the measured scattered photon energy for all types of particleboards and water was almost same to each other as shown in Figure 6 and Figure 7.

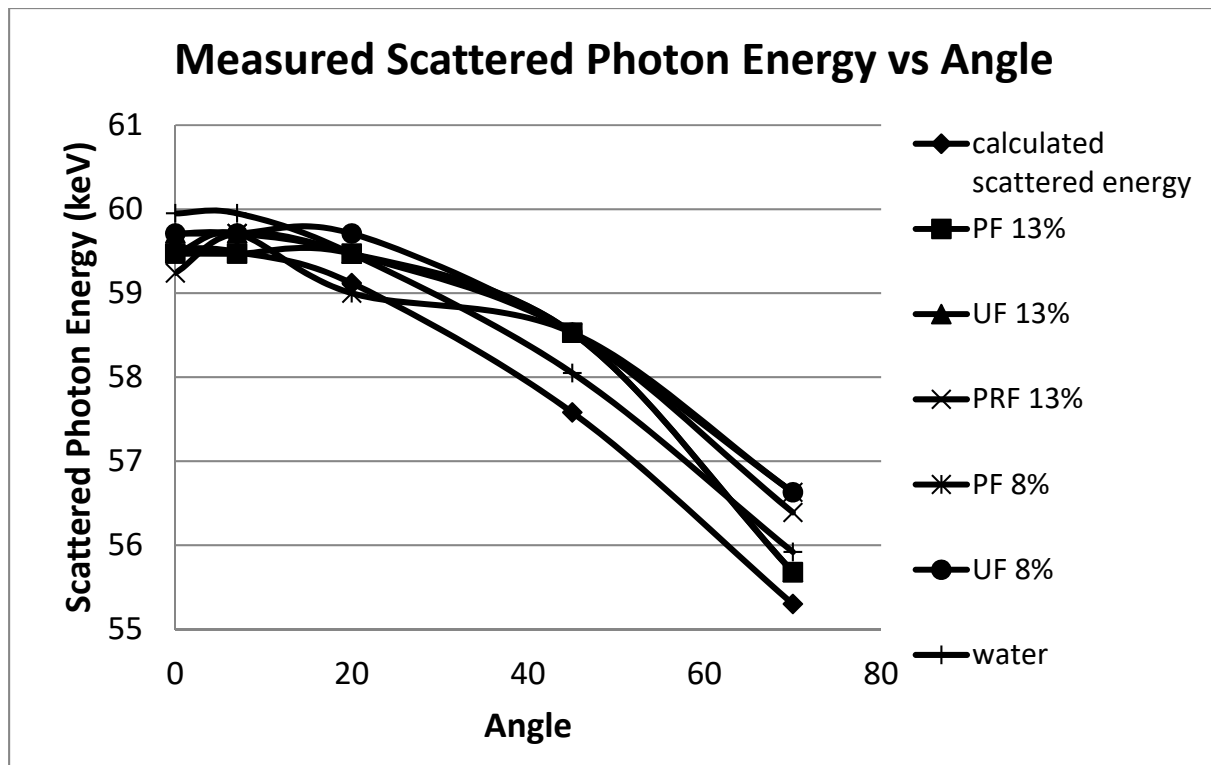


Fig. 7: Graph of measured scattered photon energy with increasing angle of scattering for all of Particle B compared with water.

D. Intensity (count per second)

Direct measurement of the intensity was obtained by measuring the area under the peak (summation of the count under peak) after subtraction of the background by using Microsoft Excel. But due to time constraint during data collection, the duration of counting was different for different angle of scattering. So, in order to differentiate the intensity of the samples for different angles of scattering, the count rate which is count under peak divided by the time of counting (in second) was used. Exponential relationships were obtained over the range of samples for different scattering angles (excluded 0°). Large angle of scattering produce less count rate (transmitted intensity low) while small angle of scattering produce high count rate (transmitted intensity high). This is because, large angle of scattering will scatter most of the incident intensity and most of them cannot be detected by the detector while small angle of incidence scatter a little of the incident intensity and most of them can be detected by the detector.

For coherent scattering, the degree of scattering varies as a function of the ratio of the particle diameter to the wavelength of the radiation, along with many other factors including polarization, angle, and coherence. Thus, difference particle diameter will cause different degree of scattering. However, cps at 0° in Table 4 and Table 5 for all of the samples was same which is in the narrow range of 2652.55 - 2742.06 cps except for water. Cps at 0° in water was the lowest than other samples which is 535.0354 cps. Otherwise, it was a little bit higher in water at 7° which is 1.04063 cps and it was the same for all of the particleboards which is around 0.61 - 0.76 cps. The reading was also the same for all of the samples at 20° and 45° but it was about 30% higher in Particle A than in Particle B. However, at 70° , cps was

around 0.10 – 0.15 cps for all samples. Overall, in Figure 8 and Figure 9 we can see that all particleboards exhibit count per second value in between water.

Table 4: Table of the count per second (cps) with increasing angle of scattering for Particle A and water.

Angle (°)	PF 13%	UF 13%	PRF 13%	PF 8%	UF 8%	Water
0	2716.45	2691.48	2680.6	2742.06	2684.28	535.0354
7	0.66083	0.70749	0.66736	0.75826	0.74104	1.04063
20	0.39188	0.36253	0.40635	0.34934	0.33913	0.38281
45	0.22544	0.20246	0.23133	0.19528	0.2023	0.26171
70	0.14824	0.13088	0.12386	0.11483	0.1279	0.12356

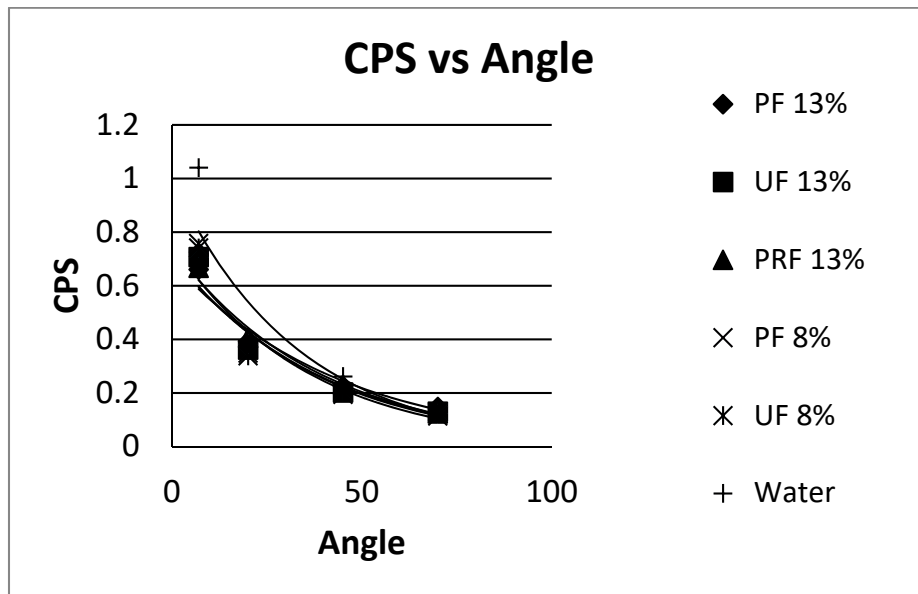


Fig. 8: Graph of count per second (cps) with increasing angle of scattering for all of Particle A compared with water.

Table 5: Table of the count per second (cps) with increasing angle of scattering for Particle B and water.

Angle (°)	PF 13%	UF 13%	PRF 13%	PF 8%	UF 8%	Water
0	2702.7	2669.99	2652.55	2723.25	2682.94	535.0354
7	0.65813	0.68417	0.63701	0.61042	0.62771	1.04063
20	0.32688	0.32313	0.36719	0.31299	0.32906	0.38281
45	0.2048	0.21597	0.23794	0.19143	0.20893	0.26171
70	0.12275	0.13351	0.13715	0.12176	0.11696	0.12356

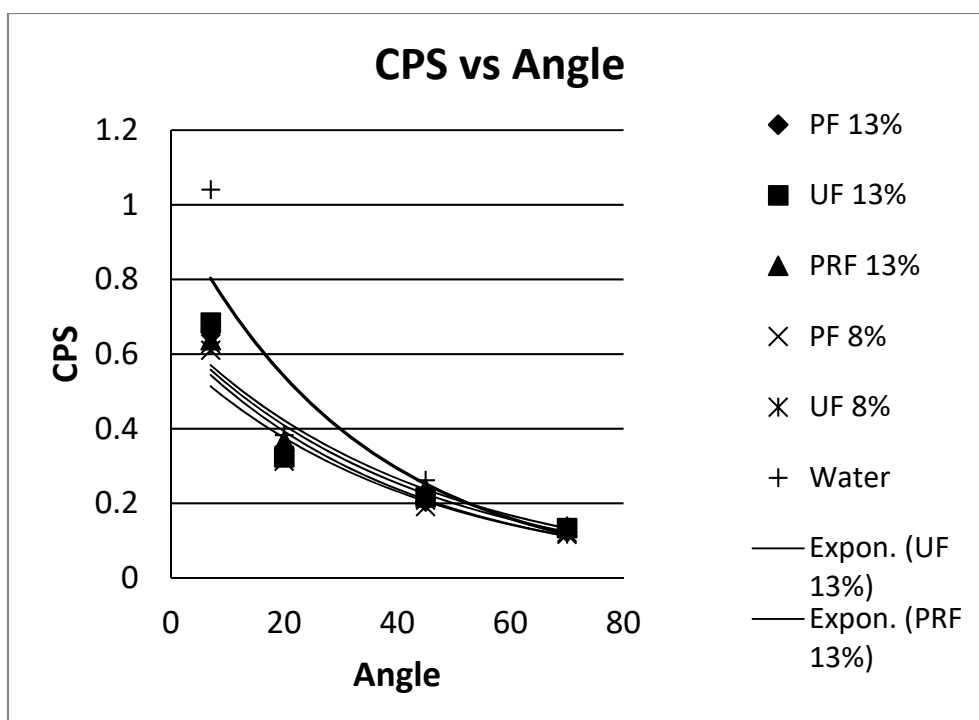


Fig. 9: Graph of count per second (cps) with increasing angle of scattering for all of Particle B compared with water.

Actually, Compton Effect depends indirectly on density [2]. But, in this study it should not affect the reading very much as all the *Rhizophora* spp. particleboards has the same density which is 0.65 g/cm^3 except for water which has a little big higher density than the particleboards which is 1 g/cm^3 . These discrepancies may be attributed to lower counting rates as Compton scattered photons usually have a very low intensity which cause the spectra to be noisy or highly fluctuative and the error in designating the scattering angle. Otherwise, another possibility in the case of the observed elevation in intensity is Bragg reflection within this range of scattering angles.

This findings are in good agreement with the investigation of this wood by Tajuddin et al. 1996 [1] that was done by using a $1.67 \text{ GBq } ^{241}\text{Am}$ source and a 5 cm NaI (TI) detector for eight scattering angles covering the range of 10° till 45° . They obtained linear relationships over the range of sample densities with progressive variation in gradient for different scattering angles. He found that decrease in scattering angle will increase in scattering intensity which supports the expected forward scattering distribution. Result of radiographic measurement also showed the mean optical densities for water given by 0.97 ± 0.02 closer to *Rhizophora* spp. with value 0.96 ± 0.02 compared to modified rubber with value 0.95 ± 0.02 . So, he concluded that *Rhizophora* spp has a similar scattering and radiographic properties to that of water and modified rubber.

IV. CONCLUSION

In this study, overall we can see that all particleboards fabricated using different types of resin materials have the same scattering properties as their channel shift, measured scattered photon energy, and count per second were almost the same. Thus, we can say that types of resin

materials do not affect much the scattering properties of *Rhizophora* spp. particleboards and these particleboards have quite same scattering properties as water in term of channel shift, measured scattered photon energy, and intensity. As for conclusion, *Rhizophora* spp. particleboard has the potential to be a water equivalence material after considering the limitations.

Acknowledgements

This work was supported by the Universiti Sains Malaysia Research University (RU) research grant number RU1001/PJJAUH/813007.

-
- [1] A.A. Tajuddin, C.W.A. Che Wan Sudin and D.A. Bradley, 'Radiographic and scattering investigation on the suitability of *Rhizophora* spp. as tissue equivalent medium for dosimetric study', *Radiat. Phys. Chem.* 47 (1996), pp. 739 – 740.
- [2] F.M. Khan, *The Physics of Radiation Therapy* 2nd Edition, Lippincott Williams & Wilkins (1994).
- [3] J.R. Williams, and D.I. Thwaites, *Radiotherapy Physics in Practice*. Oxford University Press, Oxford (2000), pp. 332.
- [4] B. Demir, H. Bilge, F.O. Dincbas, A. Koca, S. Karacam and B. Gunhan, 'The effect of pull back technique on dose distribution in the junction region for ⁹⁰Sr/⁹⁰Y intravascular brachytherapy sources', *Radiat Meas.* 39 (2005), pp. 29-32.
- [5] ICRU (International Commission on Radiation Units and Measurements). *Tissue substitutes in radiation dosimetry and measurement*. Report 44, International Commission on Radiation Units and Measurements, Bethesda, MD, USA (1989).
- [6] P. Andreo, D.T. Burns, K. Hohlfield, M.S. Huq, T. Kanai, F. Laitano, V. Smyth, S. Vynckier, 'Absorbed dose determination in external beam radiotherapy, an international code of practice for dosimetry based on standards of absorbed dose to water', *Technical Report Series No. 398*, International Atomic Energy Agency, Vienna (2000).
- [7] R.F. Hill, S. Brown and C. Baldock, 'Evaluation of water equivalence of solid phantoms using gamma ray transmission measurements', *Radiat Meas.* 43 (2008), pp. 1258 – 1264.
- [8] C.W.A. Che Wan Sudin, 'Kayu tropika sebagai bahantara setaraan tisu untuk kajian dosimetry', M.Sc. Dissertation, University of Sains Malaysia (1993).
- [9] D.P. Banjade, A.A. Tajuddin and A. Shukri, 'A study of *Rhizophora* spp. wood phantom for dosimetric purposes using high-energy photon and electron', *Appl. Radiat. Isot.* 55 (2001), pp. 297 – 302.
- [10] J.S. Al-Bahri and N.M. Spryou, 'Electron density of normal and pathological breast tissues using a Compton scattering technique' *Apl. Radiat Isot.* 49 (1999), pp. 1677 – 1684.
- [11] I. Surani, 'The suitability of PF, UF and PRF resin in term of structure and attenuation properties to be used in *Rhizophora* spp. particleboard phantoms', M.Sc. Dissertation, School of Physics, Universiti Sains Malaysia (2008).
- [12] N.A. Hussein, A. Shukri, A.A. Tajuddin, and C.S. Chong, 'LAXS investigation of finger phantoms', *Radiat. Phys. Chem.* 71 (2004), pp. 1077 – 1086.